



Figures and figure supplements

Age-related islet inflammation marks the proliferative decline of pancreatic beta-cells in zebrafish

Sharan Janjuha *et al*

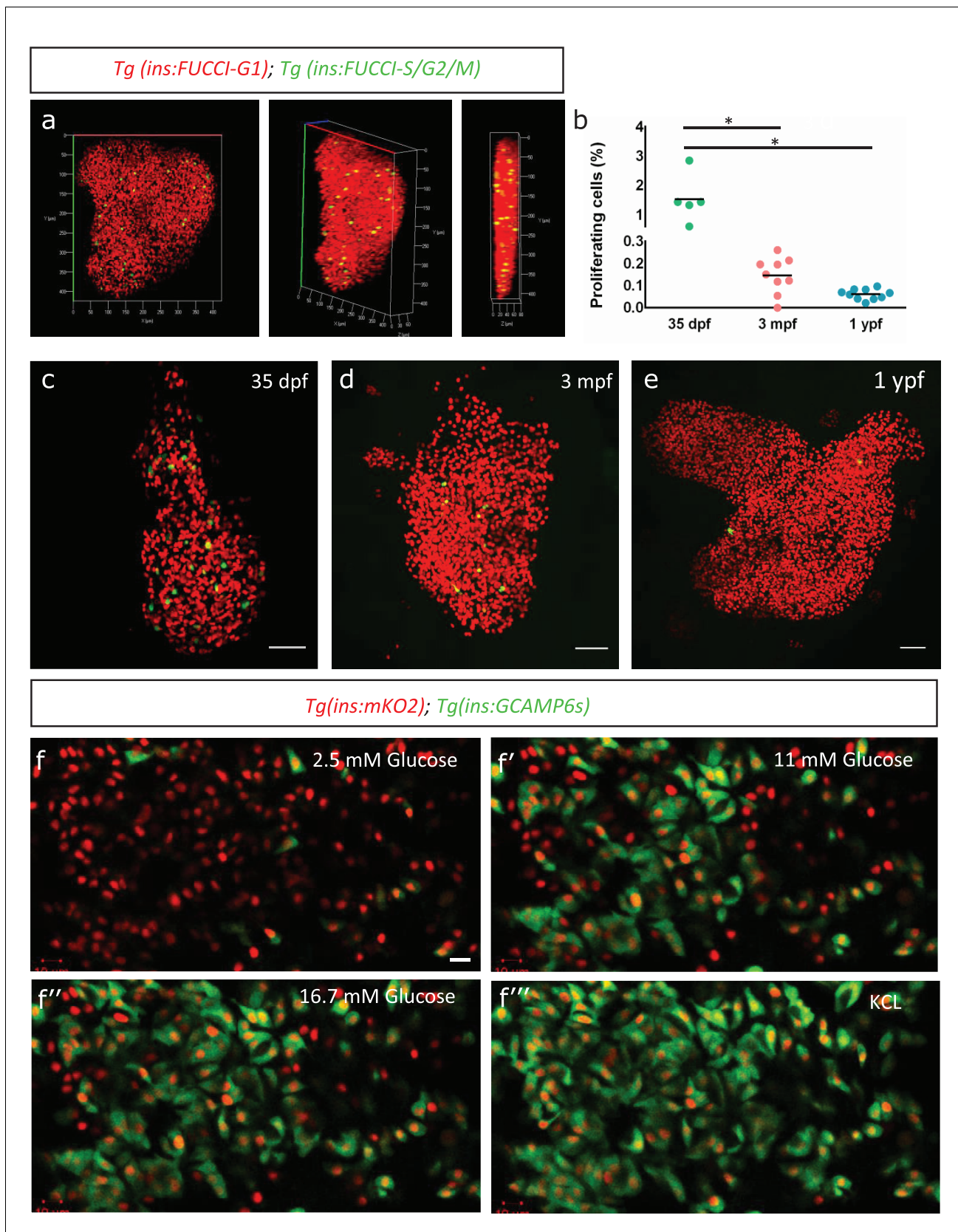
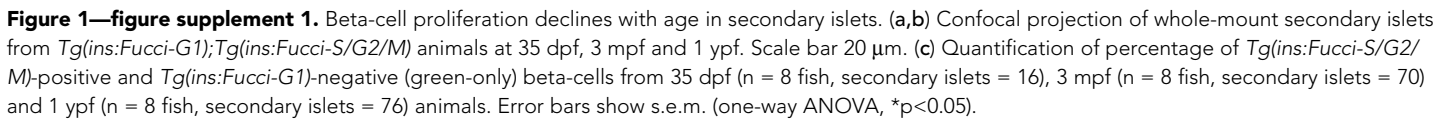


Figure 1. Beta-cell proliferation declines with age. (a) 3D-rendering of a primary islet from *Tg(ins:Fucci-G1);Tg(ins:Fucci-S/G2/M)* animals at 3 mpf showing nuclear *Tg(ins:Fucci-G1)* (red) and *Tg(ins:Fucci-S/G2/M)* (green) expression. (b) Quantification of percentage of *Tg(ins:Fucci-S/G2/M)*-positive cells. Figure 1 continued on next page

Figure 1 continued

and *Tg(ins:Fucci-G1)*-negative (green-only) beta-cells at 35 dpf (n = 5), 3 mpf (n = 9) and 1 ypf (n = 10) animals. Each dot represents one animal. Horizontal bars represent mean values (one-way ANOVA, *p<0.05). (c, d, e) Confocal projection of whole-mount islets from *Tg(ins:Fucci-G1);Tg(ins:Fucci-S/G2/M)* animals at 35 dpf, 3 mpf and 1 ypf. Anterior to the top. Scale bar 50 μ m. (f) Ex vivo live-imaging of beta-cells from *Tg(ins:nlsRenilla-mKO2);Tg(ins:GCaMP6s)* animals at 3 mpf. Beta-cells (red) were stimulated with 2.5 (basal) mM D-Glucose, (f') 11 mM D-glucose, (f'') 16.7 mM D-glucose and (f''') depolarized using 30 mM KCl while monitoring GCaMP6s-fluorescence (green). Scale bar 10 μ m.

DOI: <https://doi.org/10.7554/eLife.32965.002>



Janjuha et al. eLife 2018;7:e32965. DOI: <https://doi.org/10.7554/eLife.32965>

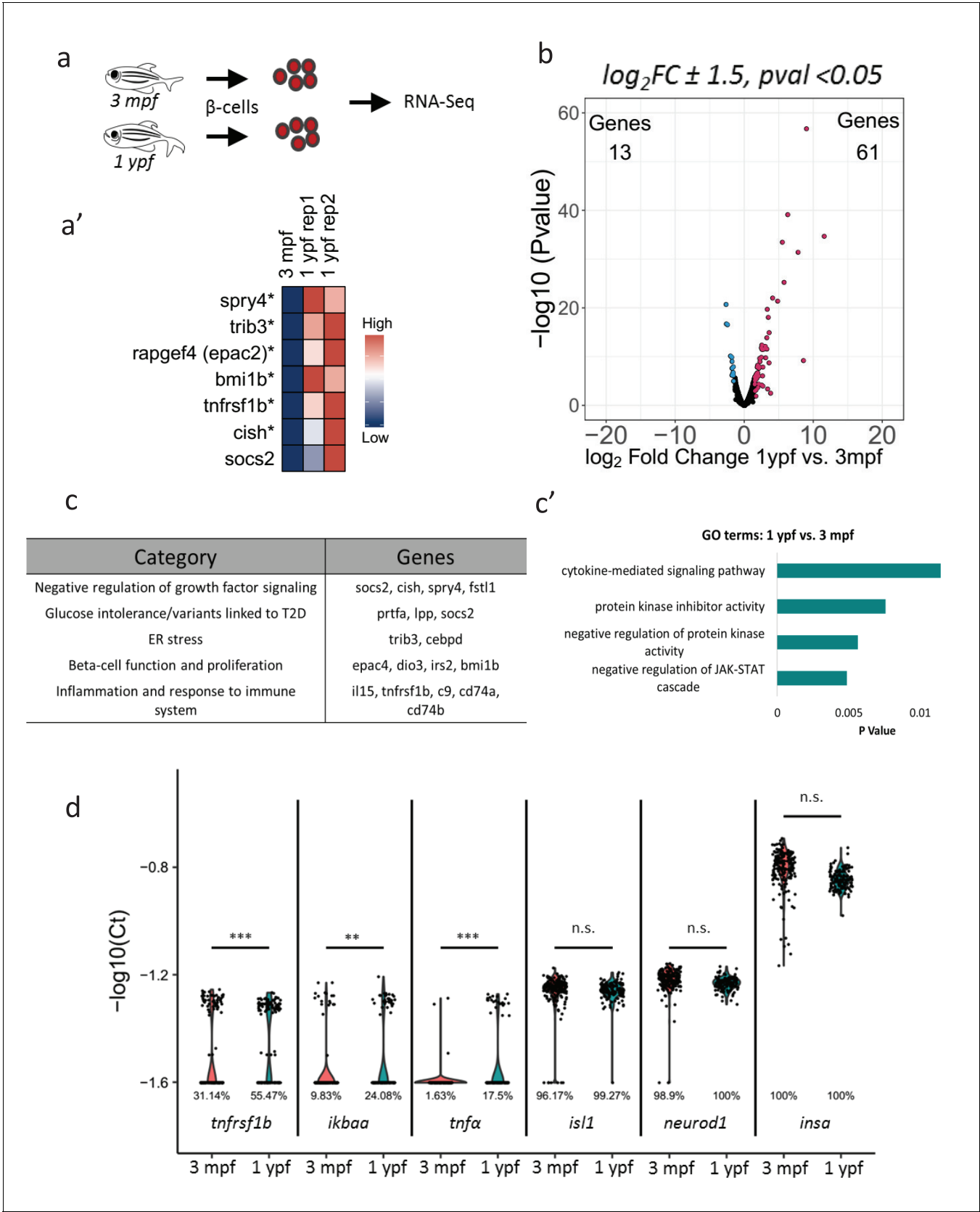


Figure 2. Transcriptome profiling of younger and older beta-cells. (a) Schematic showing isolation and FAC-sorting of beta-cells from *Tg(ins:nlsRenilla-mKO2)* animals at 3 mpf and 1 ypf followed by high-throughput mRNA-Sequencing. (a') Heatmap depicting differentially regulated genes among the

Figure 2 continued on next page

Figure 2 continued

beta-cells at 1 ypf and 3 mpf involved in beta-cell proliferation, function and inflammation (asterisks denote genes validated by single-cell RT-qPCR). (b) Volcano plot representing the distribution of genes that were differentially regulated in beta-cells from 1 ypf and 3 mpf (1.5- \log_2 fold change, $p < 0.05$). (c) The biological categories of enriched genes in beta-cells at one ypf (1.5- \log_2 fold change, $p < 0.05$) based on literature survey. (c') Unbiased gene-ontology analysis using DAVID of genes enriched in beta-cells at 1 ypf ($p < 0.05$). (d) Gene expression analysis was carried out using single-cell RT-qPCR. Violin plots denote expression distribution of the candidate genes. The Y-axis shows $-\log_{10}(\text{Ct})$ values of transcript levels in single beta-cells. The X-axis shows gene names and the respective developmental stages. The percentage values under each violin plot denote the proportion of beta-cells with detectable transcript levels. The cycle threshold for detectable gene expression was set as $\text{Ct} = 40$. The value -1.6 ($-\log_{10}(40)$) on the Y-axis represents undetectable expression as measured by single-cell RT-qPCR (see Materials and methods). Each dot represents one beta-cell. Significance testing for differences in proportion of cells with detectable gene expression at each stage was performed using Pearson's Chi-Square test (** $p < 0.01$, *** $p < 0.001$).

DOI: <https://doi.org/10.7554/eLife.32965.004>

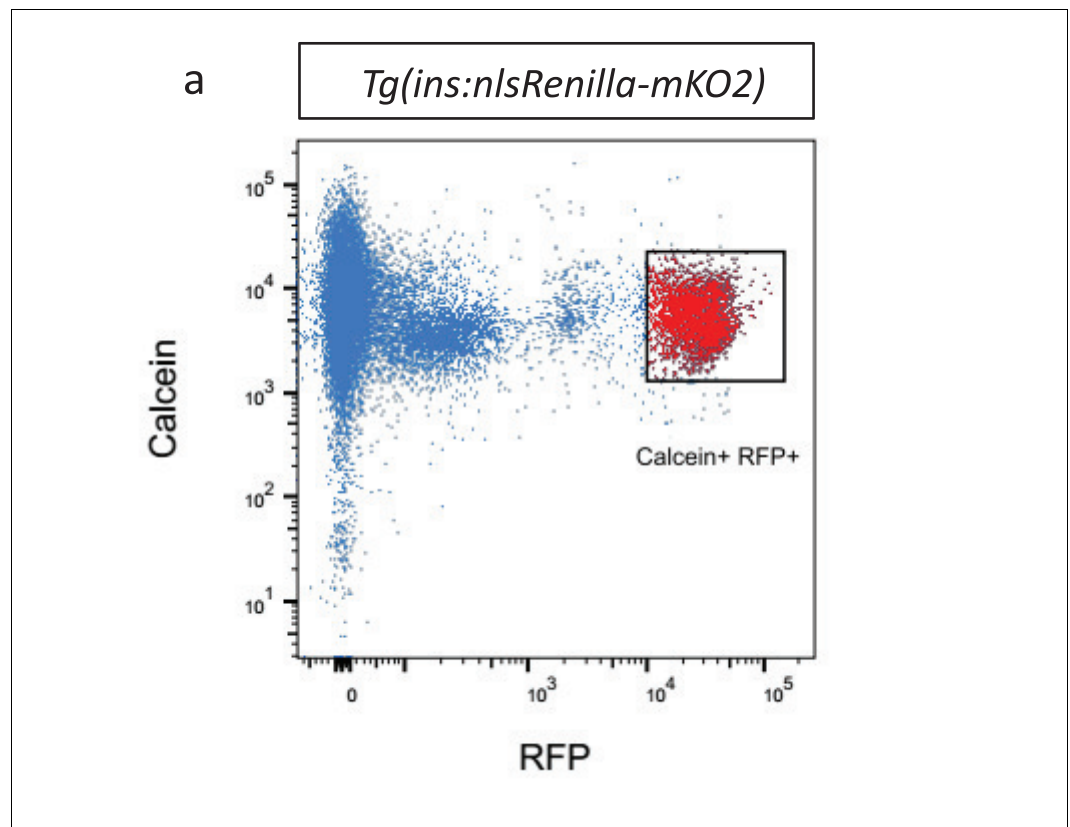


Figure 2—figure supplement 1. Fluorescent activated cell sorting of beta-cells. (a) Fluorescent activated cell sorting (FACS) of RFP-positive and calcein-positive beta-cells from *Tg(ins:nlsRenilla-mKO2)* animals.

DOI: <https://doi.org/10.7554/eLife.32965.005>

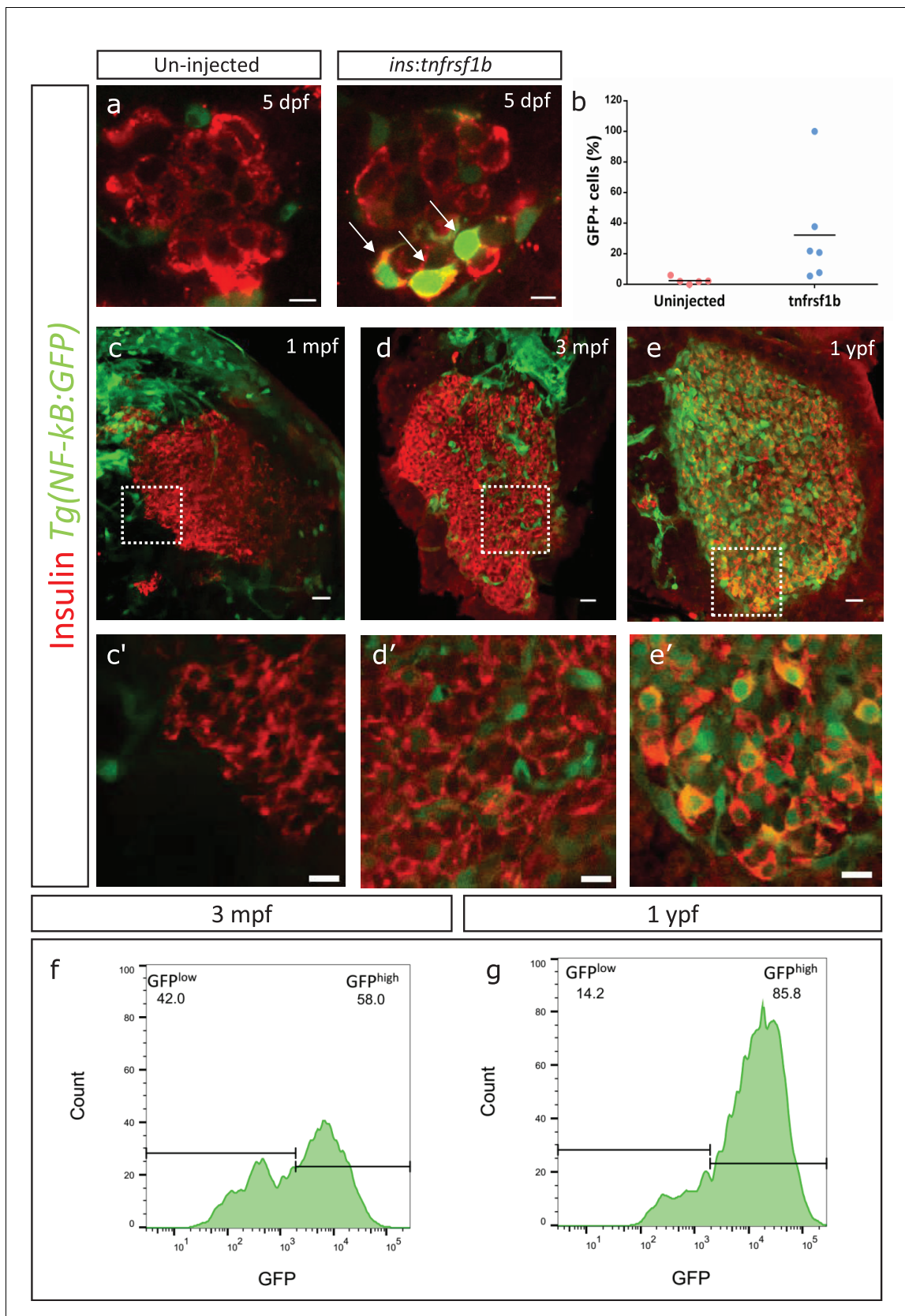


Figure 3. An inflammation reporter reveals heterogeneous activation of NF- κ B signaling in beta-cells with age. (a) The images show single confocal planes from islets of 5 dpf larvae. The *tnfrsf1b* coding sequence was expressed under the control of the insulin promoter. The plasmid was injected in

Figure 3 continued on next page

Figure 3 continued

Tg(NF- κ B:GFP) embryos at the one-cell-stage, leading to mosaic and stochastic expression of the construct in beta-cells. The *Tg(NF- κ B:GFP)* reporter expresses GFP (green) under the control of six tandem repeats of NF- κ B DNA-binding sites. Beta-cells were labelled using an insulin antibody (red). Arrows indicate GFP-positive beta-cells. Scale bar 5 μ m. (b) The graph shows the percentage of GFP-positive and insulin-positive cells in uninjected controls (n = 5) and *tnfrsf1b* injected animals (n = 6) at 5 dpf. Horizontal bars represent mean values. (c–e) Confocal stack of islets from *Tg(NF- κ B:GFP)* animals at 1 mpf, 3 mpf and 1 ypf. Beta-cells were labeled using an insulin antibody (red). NF- κ B:GFP reporter expression is shown in green. Scale bars 20 μ m. (c'–e') Insets show high magnification single planes of the confocal stacks (corresponding to the regions shown using white dotted-lines in the top panels). Scale bar 10 μ m. (f–g) Beta-cells from 3 mpf *Tg(NF- κ B:GFP)* animals were labeled with TSQ (Zn²⁺ labeling dye) and analyzed using FACS. The graph shows GFP intensity (along the X-axis) and the distribution of beta-cells at 3 mpf and 1 ypf. Horizontal lines indicate the division point between GFP^{low} and GFP^{high} levels. Percentage values represent proportion of cells with GFP^{low} or GFP^{high} expression.

DOI: <https://doi.org/10.7554/eLife.32965.006>

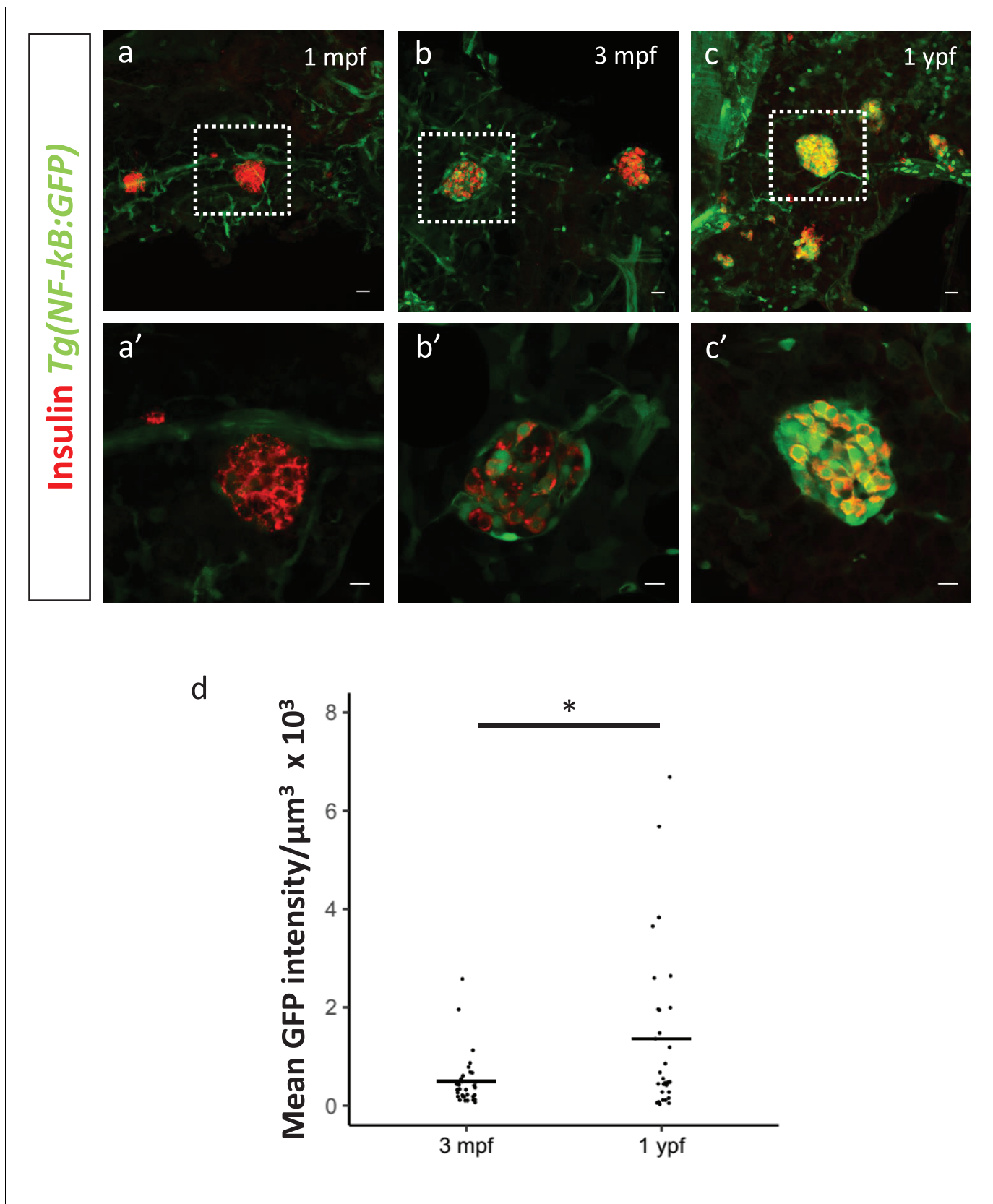


Figure 3—figure supplement 1. Activation of NF- κ B signaling in beta-cells of the secondary islets with age. (a,b,c) Confocal stack of secondary islets from *Tg(NF- κ B:GFP)* animals at 1 mpf, 3 mpf and 1 ypf. Beta-cells were labeled using an insulin antibody (red). NF- κ B:GFP reporter expression is shown in green. *Figure 3—figure supplement 1 continued on next page*

Figure 3—figure supplement 1 continued

in green. Scale bars 20 μm . (a',b',c') Insets show high-magnification single planes of the confocal stacks corresponding to the regions outlined using white dotted-lines in the top panels. Scale bar 10 μm . (d) Graph showing the total normalized GFP fluorescence intensity of the secondary islets from 3 mpf (n = 9 fish, secondary islets = 32) and 1 ypf (n = 8, secondary islets = 30) animals. Each dot represents one islet (two-tailed t-test, *p<0.05). DOI: <https://doi.org/10.7554/eLife.32965.007>

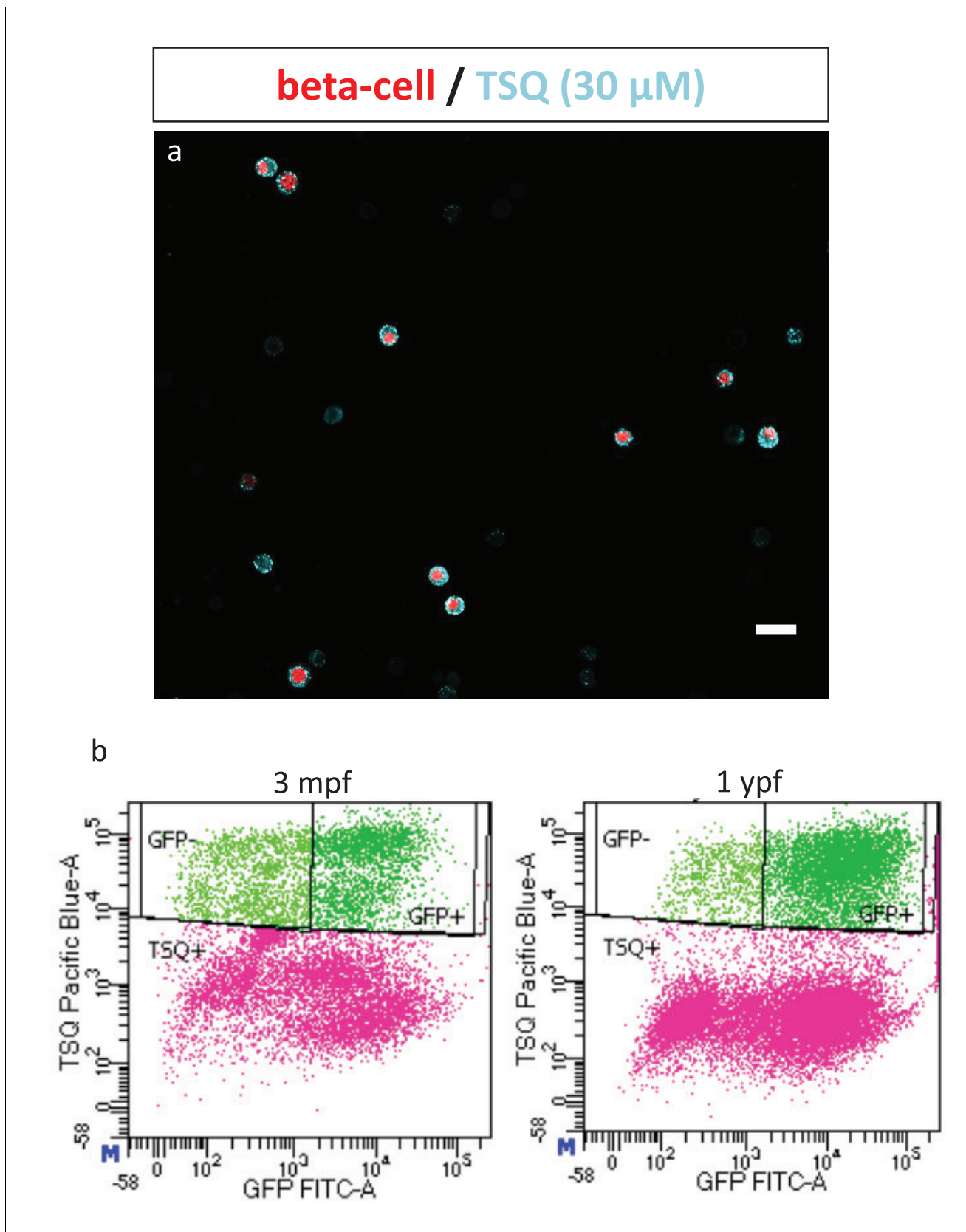


Figure 3—figure supplement 2. Fluorescent activated cell sorting of $NF-\kappa B:GFP^{high}$ and $NF-\kappa B:GFP^{low}$ beta-cells. (a) Confocal image of dissociated cells from dissected islets of 3 mpf *Tg(ins:nlsRenilla-mKO2)* animals that were labeled with TSQ (Zn^{2+} labeling dye). Islets were incubated with TSQ after Figure 3—figure supplement 2 continued on next page

Figure 3—figure supplement 2 continued

dissociation and imaged using a confocal microscope. Beta-cells show RFP expression (red) while cells rich in Zn^{2+} are labeled with TSQ (cyan). TSQ strongly labels all beta-cells and weakly labels some unknown endocrine cells. **(b)** Fluorescent activated cell sorting (FACS) of live TSQ-positive GFP^{high} and GFP^{low} cells from *Tg(NF- κ B:GFP)* animals at 3 mpf and 1 ypf. Dead cells were labelled using far-red stain DRAQ7.

DOI: <https://doi.org/10.7554/eLife.32965.008>

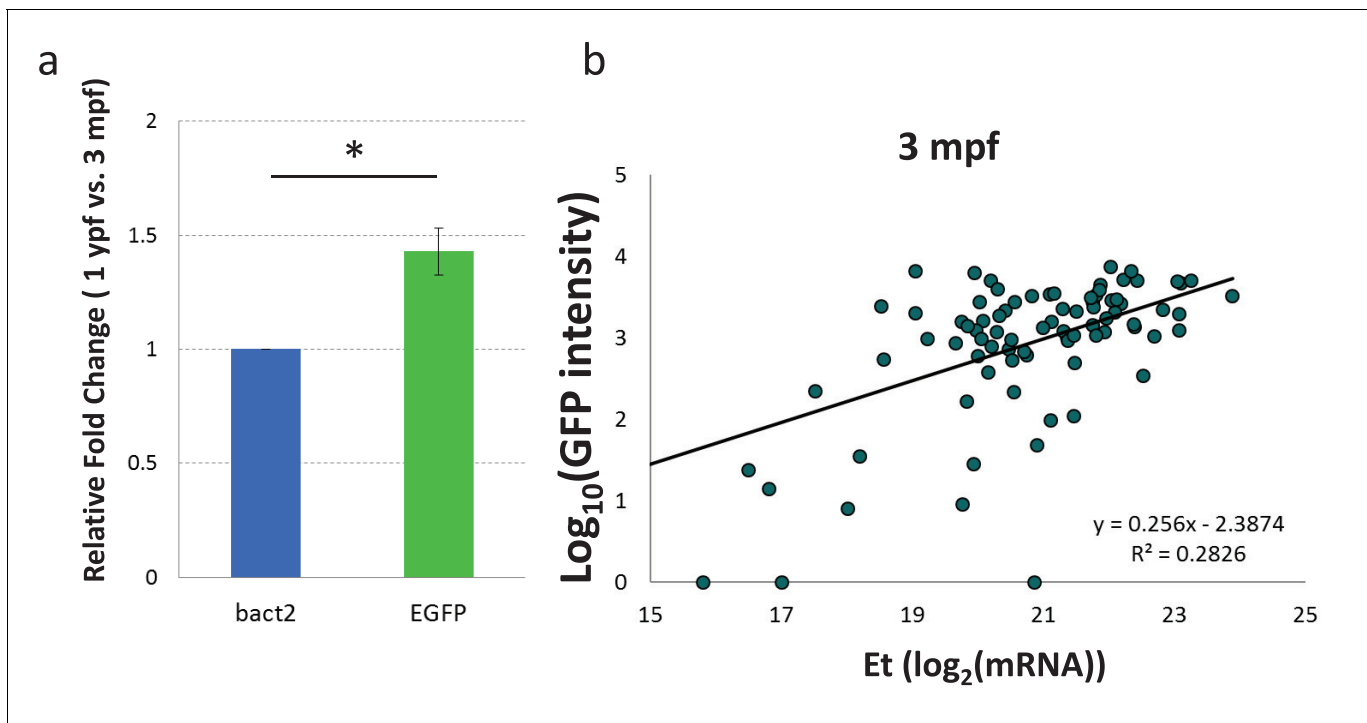


Figure 3—figure supplement 3. *NF-κB:EGFP* mRNA levels in beta-cells increase with age. (a) Graph showing the relative fold change increase in EGFP mRNA levels in beta-cells from 1 ypf compared to 3 mpf animals, as measured using RT-qPCR (n=5 biological replicates from three fish each, 1000 cells for each condition). Error bars show SD (two-tailed paired t-test, *p<0.05). (b) The graph shows the fluorescence levels of individual FAC-sorted beta-cells from *Tg(nF-κB:GFP);Tg(ins:mCherry)* animals as log₁₀(GFP intensity) (along the Y-axis) and Expression threshold (Et) values of GFP mRNA (along X-axis) measured using single-cell RT-qPCR. Line indicates the correlation between GFP fluorescence intensity and GFP-mRNA expression levels in single cells. Each dot represents one beta-cell. $R^2 = 0.28$.

DOI: <https://doi.org/10.7554/eLife.32965.009>

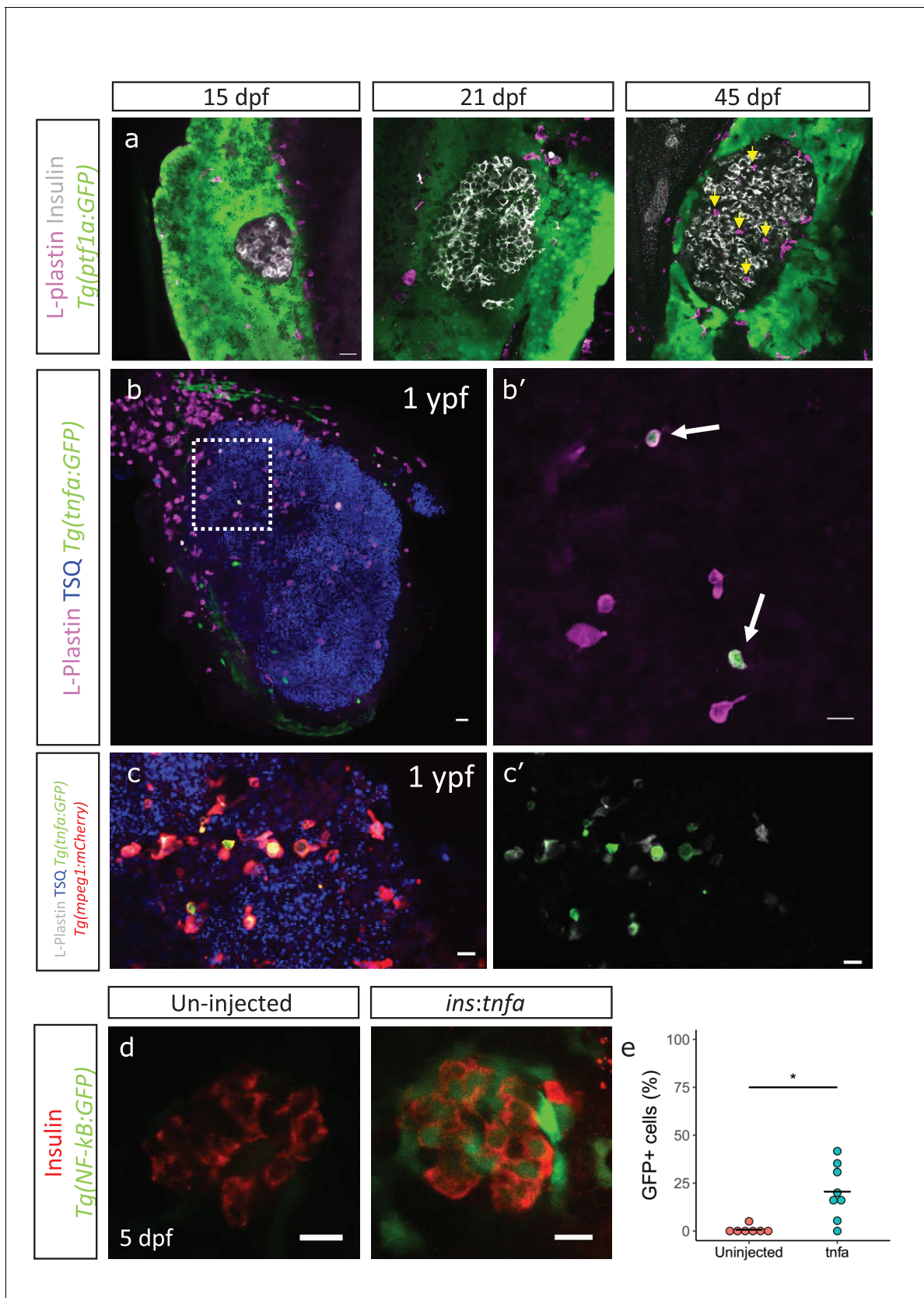


Figure 4. Immune cells infiltrate the islet during development and persist throughout adult life. (a) Confocal images of pancreata from 15, 21 and 45 dpf animals. Beta-cells were labeled using an insulin antibody (grey), leukocytes were labeled using an L-plastin antibody (magenta) and *Tg(ptf1a:GFP)* Figure 4 continued on next page

Figure 4 continued

marks the acinar cells (green). Immune cells are present within the islet at 45 dpf (arrows). (b) Confocal images of whole islets from *Tg(tnfa:GFP)* animals at 1 ypf. Islets were labeled using TSQ (Zn^{2+} labeling dye) (blue), leukocytes were labelled with an L-plastin antibody (magenta) and *Tg(tnfa:GFP)* marks cells expressing *tnfa* (green). Scale bars 20 μm . (b') Insets show high-magnification single planes from the confocal stacks (corresponding to the area marked using a white dotted-line in b). Scale bar 10 μm . (c–c') Confocal image of a one ypf islet showing a single plane. The *TgBAC(tnfa:GFP)* line marks the *tnfa*-positive cells (green), whereas *Tg(mpeg1:mCherry)* marks the macrophages (red). The L-plastin antibody marks all leukocytes (grey) and TSQ (Zn^{2+} labeling dye) was used to mark the islet ($n = 5$). Scale bar, 10 μm . (d) Confocal images showing islets at five dpf. The *tnfa* cDNA was expressed under the insulin promoter. The plasmid was injected in *Tg(NF-kB:GFP)* embryos at the one-cell-stage and the islets were analyzed at 5 dpf. Beta-cells were labeled with an insulin antibody (red). *Tg(NF-kB:GFP)* reporter expression is shown in green. (e) The graph shows the percentage of GFP and insulin double-positive cells in un-injected controls ($n = 7$) and *ins:tnfa* injected animals ($n = 8$) at five dpf. Horizontal bars represent mean values (two-tailed t-test, $*p < 0.05$).

DOI: <https://doi.org/10.7554/eLife.32965.010>

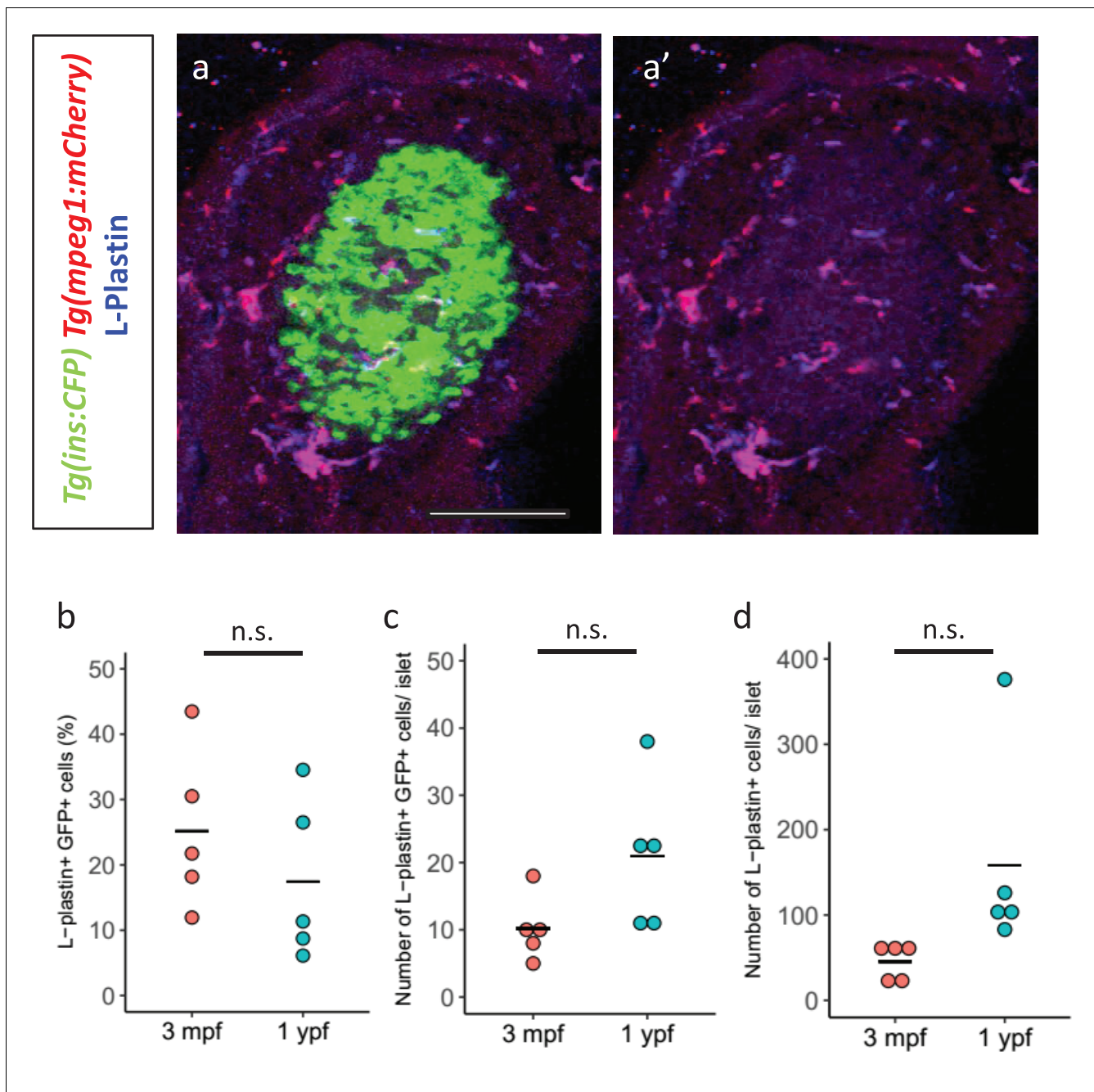


Figure 4—figure supplement 1. Immune cells infiltrate the islet during development. (a,a') Confocal image of a juvenile islet. Tg(*ins:CFP-NTR*) line marks the beta-cells with CFP (green), leukocytes were labelled with the L-plastin antibody (blue) and Tg(*mpeg1:mCherry*) marks the macrophages (red). (b) Quantification of the percentage of TgBAC(*tnfa:GFP*) and L-plastin double-positive cells over the total number of L-plastin-positive cells in the islets of TgBAC(*tnfa:GFP*) animals at 3 mpf (n = 5) and 1 ypf (n = 5). Horizontal bars represent mean values (two-tailed t-test, $p > 0.05$). (c) Quantification of the total number of TgBAC(*tnfa:GFP*)-positive and L-plastin double-positive cells at 3 mpf (n = 5) and 1 ypf (n = 5). Horizontal bars represent mean values (two-tailed t-test, $p > 0.05$). (d) Quantification of the total number of L-plastin positive cells at 3 mpf (n = 5) and 1 ypf (n = 5). Horizontal bars represent mean values (two-tailed t-test, $p > 0.05$).

DOI: <https://doi.org/10.7554/eLife.32965.011>

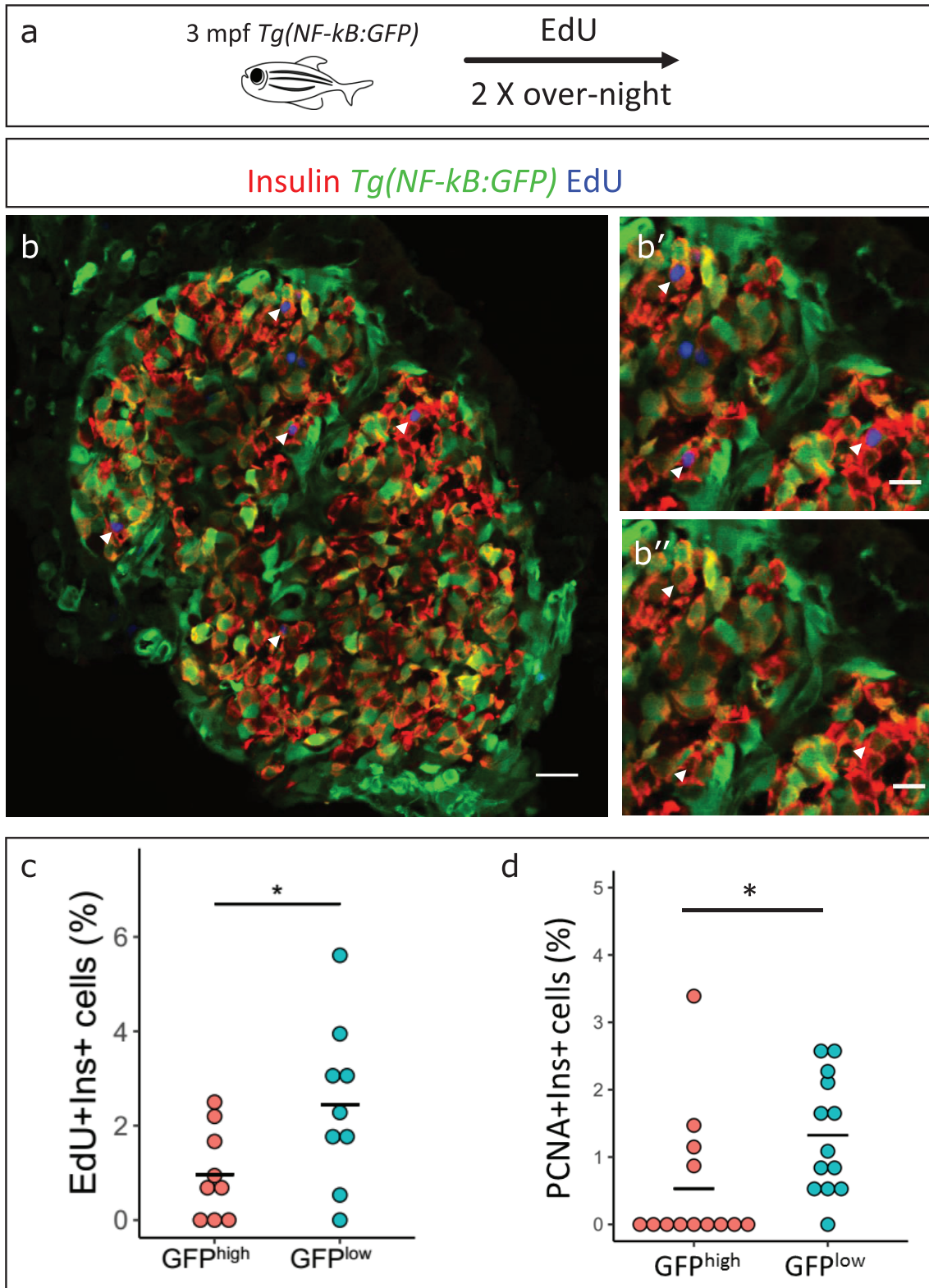


Figure 5. *NF-κB:GFP^{high}* beta-cells proliferate less than their neighbors. (a) Schematic showing the EdU (5-ethynyl-2'-deoxyuridine) incorporation assay. *Tg(NF-κB:GFP)* animals were incubated in EdU at 3 mpf for two consecutive nights and fed during each day. (b) EdU incorporation assay was performed

Figure 5 continued on next page

Figure 5 continued

to mark the proliferating beta-cells in *Tg(NF- κ B:GFP)* animals at 3 mpf. The confocal image (single plane) shows an overview of a section through the islet. Beta-cells were labeled with an insulin antibody (red), a GFP antibody (green) and EdU (blue). Arrowheads point to EdU-positive beta-cells. (**b'–b''**) The insets show higher magnification images with and without the EdU channel. EdU incorporation can be observed in some of the GFP^{low} cells (white arrow-heads). (**c**) An insulin-positive cell was first located by going through individual sections in the confocal z-stack. The optical section containing the largest area of the nucleus was chosen as the center of the cell. A region-of-interest (ROI) was drawn around the nucleus and the fluorescence intensities of the GFP and DAPI channels were recorded. The normalized GFP intensity was calculated as a ratio of mean GFP intensity and mean DAPI intensity for each ROI. The average total normalized GFP-intensity of each islet was set as a threshold for dividing the cells into GFP^{high} and GFP^{low} populations. The graph shows the percentage of EdU and insulin double-positive cells among the GFP^{high} and GFP^{low} populations. Each dot represents one islet (n = 9). Horizontal bars represent mean values (two-tailed t-test, *p<0.05). (**d**) The graph shows the percentage of PCNA and insulin double-positive cells among the GFP^{high} and GFP^{low} populations. Each dot represents one islet (n = 13). Horizontal bars represent mean values (two-tailed t-test, *p<0.05). See also **Figure 5—figure supplement 2** for representative PCNA antibody staining.

DOI: <https://doi.org/10.7554/eLife.32965.012>

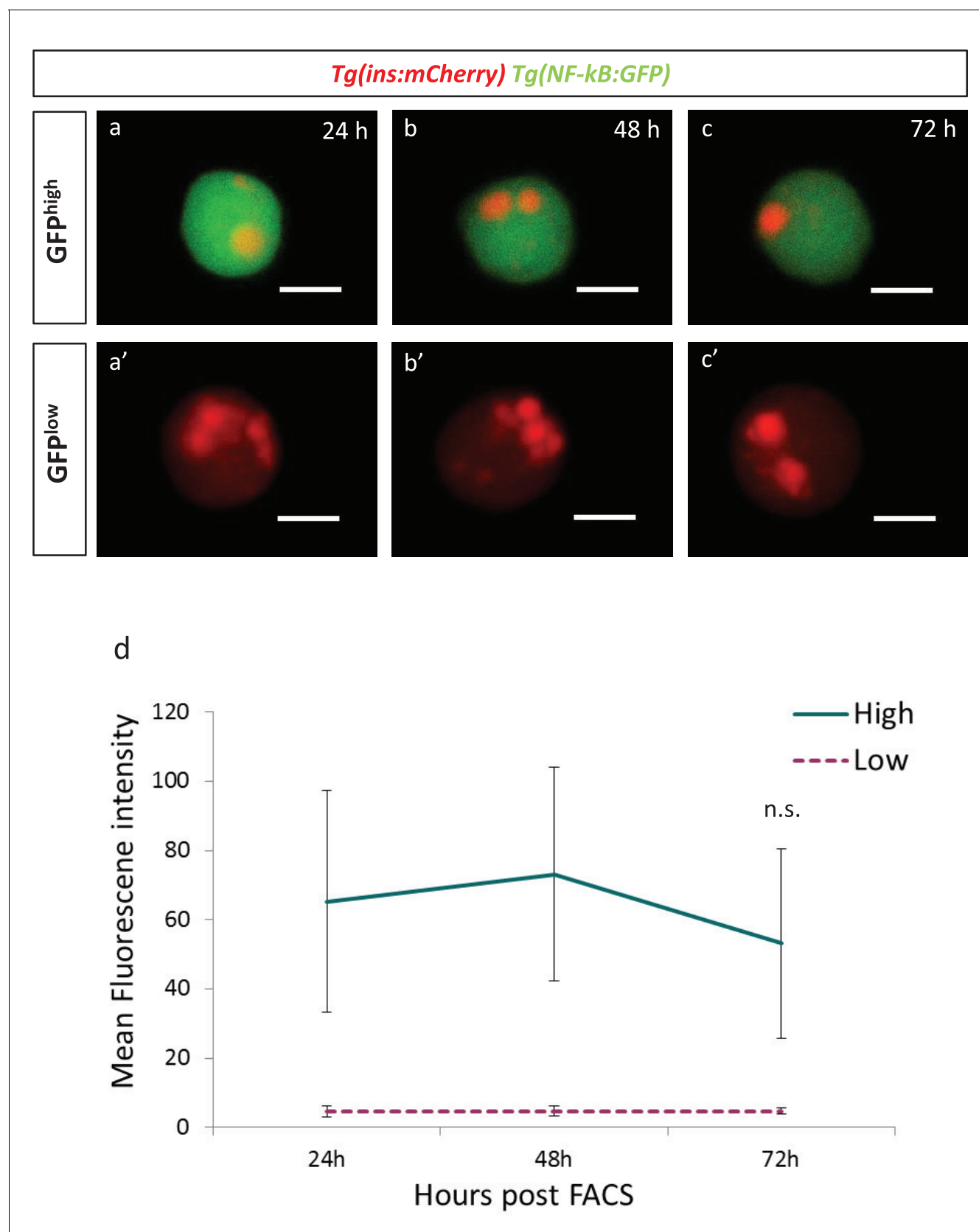


Figure 5—figure supplement 1. The GFP fluorescence of the transgenic reporter *Tg(NF-kB:GFP)* remains stable for 72 hours in beta-cells. (a,b,c) Beta-cells from *Tg(NF-kB:GFP);Tg(ins:mCherry)* animals at 3 mpf were FACS-sorted as single cells in 384-well plates and followed over 72 hr. *NF-kB:GFP^{high}*

Figure 5—figure supplement 1 continued on next page

Figure 5—figure supplement 1 continued

cells at 24, 48 and 72 hr post-FAC-sorting. Scale bar 5 μm . (a',b',c') *NF- κ B*:GFP^{low} cells at 24, 48 and 72 hr post-FAC-sorting. Scale bar 5 μm . (d) Quantification showing the mean GFP fluorescence intensity of GFP^{high} and GFP^{low} cells (n = 7 GFP^{high} cells and n = 5 GFP^{low} cells).

DOI: <https://doi.org/10.7554/eLife.32965.013>

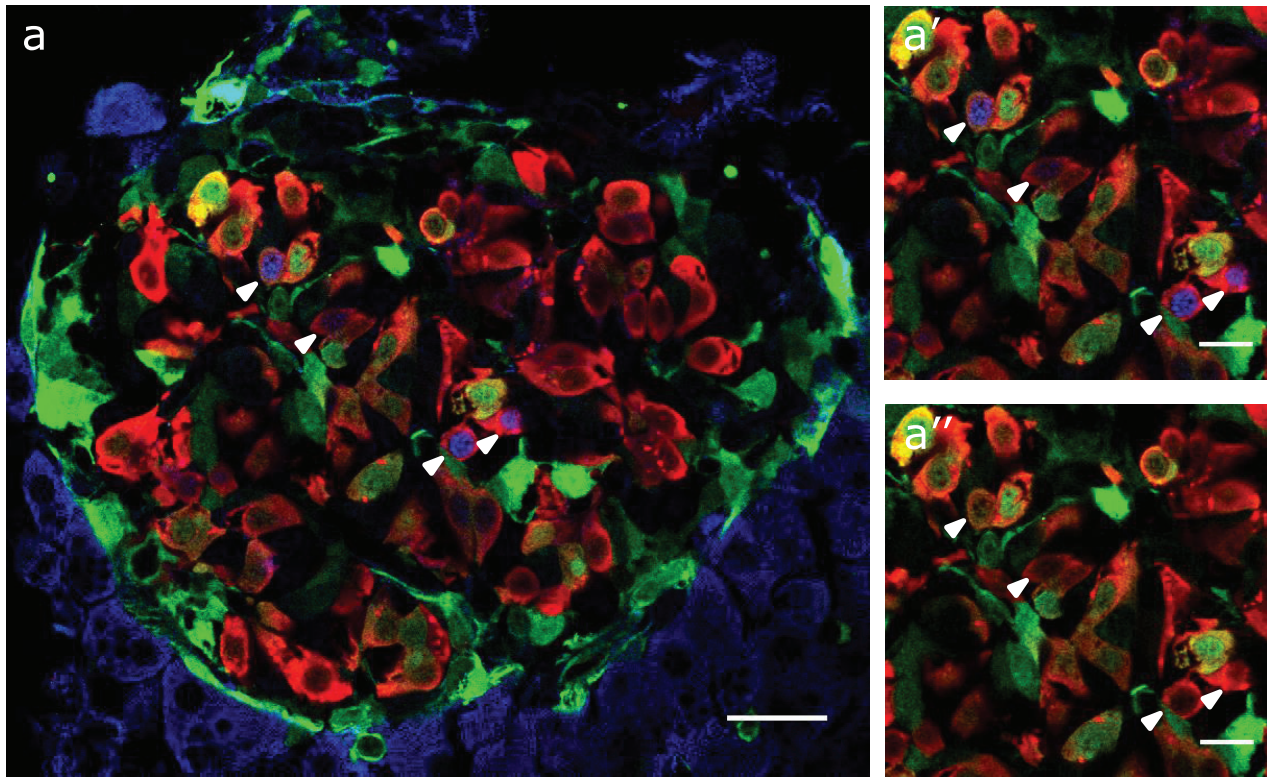
Insulin *Tg(NF-kB:GFP)* PCNA

Figure 5—figure supplement 2. Proliferating cell nuclear antigen (PCNA) antibody staining shows that *NF-kB:GF* Phighbeta-cells proliferate less than *NF-kB:GFP* low beta-cells. (a) Islets were stained for PCNA to mark the proliferating beta-cells in *Tg(NF-kB:GFP)* animals at 3 mpf. The confocal image (single plane) shows an overview of a section through the islet. The sections were stained with an insulin antibody (red), a GFP antibody (green) and PCNA (blue). (a'–a'') The insets show higher magnification images. PCNA can be observed in some of the GFP^{low} cells (white arrow-heads).

DOI: <https://doi.org/10.7554/eLife.32965.014>

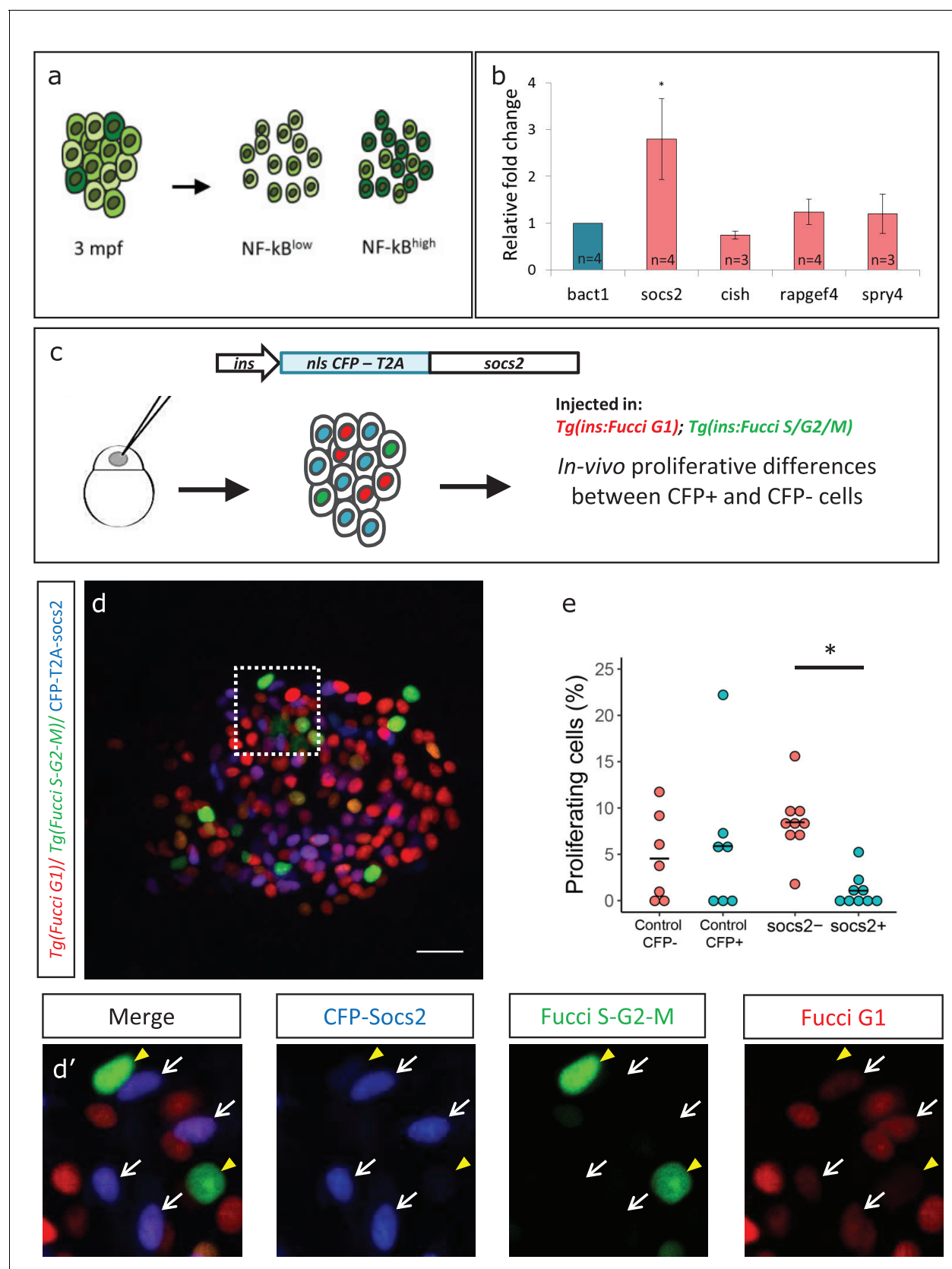


Figure 6. Socs2 is enriched in NF- κ B:GFP^{high} cells and inhibits beta-cell proliferation in a cell-autonomous manner. (a) Schematic showing the sorting of beta-cells from the double transgenic line *Tg(ins:mCherry);Tg(NF- κ B:GFP)* at 3 mpf into GFP^{high} and GFP^{low} cells using FACS. (b) Bulk RT-qPCR was performed on sorted cells. (c) Schematic of the ins promoter driving nls CFP-T2A and socs2. (d) Fluorescence microscopy image of a cell cluster. (e) Dot plot of proliferating cells (%). (d') Merged fluorescence microscopy images of CFP-Socs2, Fucci S-G2-M, and Fucci G1.

Figure 6 continued on next page

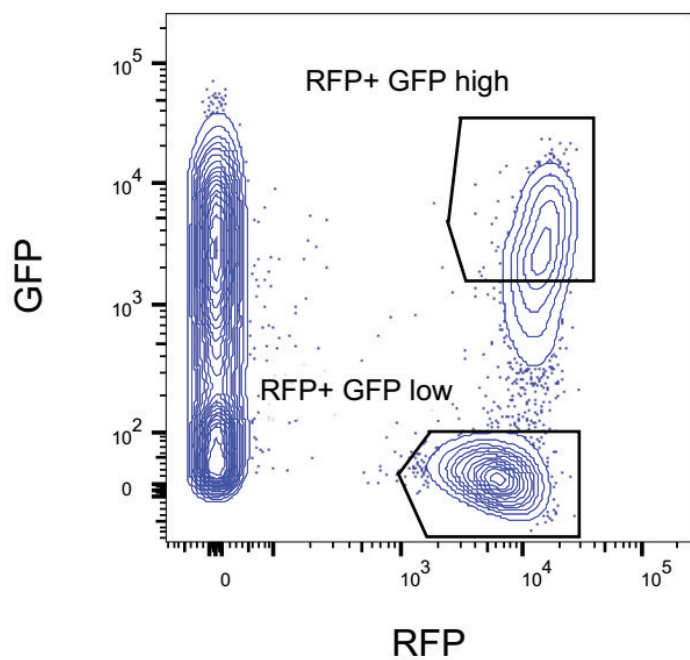
Figure 6 continued

performed on the GFP^{high} and GFP^{low} beta-cells (n = 3 to 4 biological replicates, n = 3 animals per replicate, 1000 cells per condition). Candidate genes significantly enriched in beta-cells at 1 ypf were chosen to be compared between the GFP^{high} and GFP^{low} populations at 3 mpf. The graph shows relative fold-change between GFP^{high} and GFP^{low} cells. The expression of all genes was normalized to β -actin expression before calculating fold-change. *socs2* shows higher expression in the GFP^{high} cells. Error bars, SD (two-tailed paired t-test, *p<0.05). (c) Schematic showing the method for mosaic overexpression of candidate genes in beta-cells. The *socs2* coding sequence is linked to nuclear-CFP using a T2A sequence. The entire construct was expressed under the insulin promoter. This construct was injected in one-cell-stage-embryos from *Tg(ins:Fucci-G1);Tg(ins:Fucci-S/G2/M)* animals leading to mosaic and stochastic expression of *socs2* in beta-cells during islet development. Control animals were injected with plasmid containing only nuclear-CFP sequence (See **Figure 6—figure supplement 2**). (d) Confocal projections showing mosaic expression of *socs2*-T2A-CFP (blue) at 23 dpf (blue). Proliferating beta-cells are marked by *Tg(ins:Fucci-S/G2/M)* expression (green) and absence of *Tg(ins:Fucci-G1)* expression (red). Anterior to the left. Scale bar 10 μ m. (d') Insets show higher magnification single planes from the confocal stacks (white dotted-line in d) with separate channels. The proliferating beta-cells are CFP-negative (yellow arrowheads), whereas some of the non-proliferating cells are CFP-positive (white arrowheads) (e) Quantification of the percentage of *Tg(ins:FUCCI-S/G2/M)*-positive and *Tg(ins:FUCCI-G1)*-negative (green only) beta-cells. The *socs2* expressing β -cells exhibit reduced cell-cycle progression compared to wild-type neighbors (n = 9). Horizontal bars represent mean values (two-tailed t-test, *p<0.05).

DOI: <https://doi.org/10.7554/eLife.32965.015>

Tg(ins:mCherry);Tg(NF-kB:GFP) 3 mpf

a



b

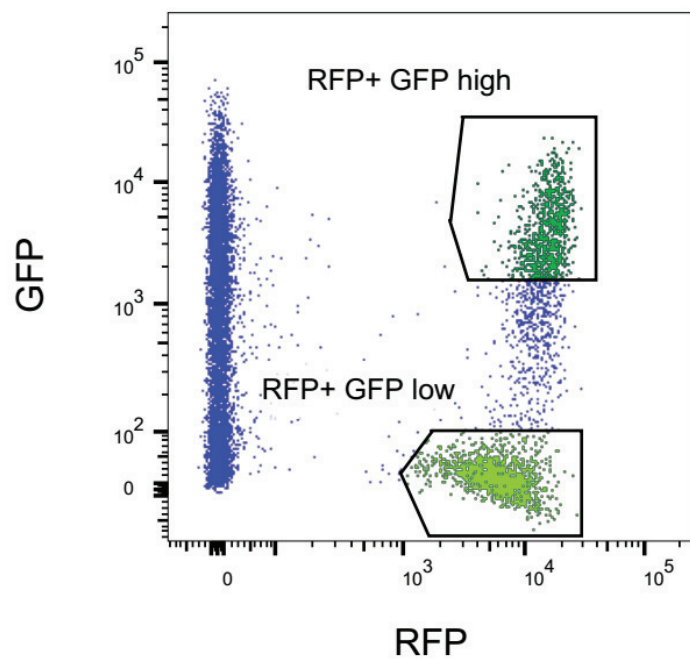


Figure 6—figure supplement 1. Fluorescent activated cell sorting of *NF-κB*:GFP^{high} and *NF-κB*:GFP^{low} beta-cells. (a) Contour plot showing FACS of live RFP-positive GFP^{high} and GFP^{low} cells from *Tg(NF-κB:GFP);Tg(ins:mCherry)* animals at 3 mpf. Live cells were labeled with calcein. (b) Dot plot shows FACS of live RFP-positive GFP^{high} and GFP^{low} cells from *Tg(NF-κB:GFP);Tg(ins:mCherry)* animals at 3 mpf.

DOI: <https://doi.org/10.7554/eLife.32965.016>

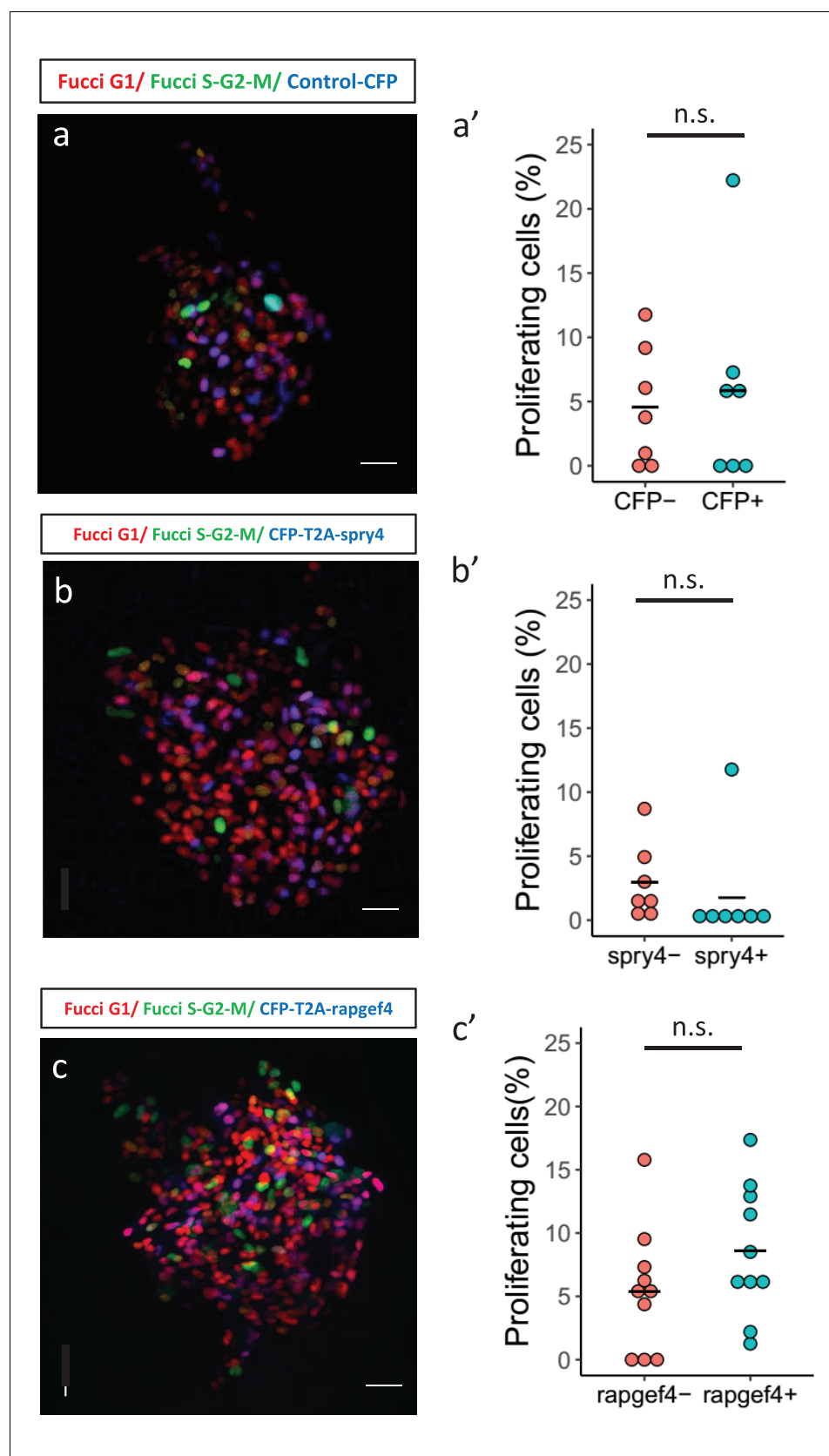


Figure 6—figure supplement 2. Mosaic expression of candidate genes in beta-cells to study their effect on proliferation. (a,b,c) Confocal images showing mosaic expression of nuclear-CFP (a), CFP-T2A-spry4 (b) and CFP-T2A-rapegef4 (c). (a',b',c') Dot plots showing the percentage of proliferating cells for each condition. n.s. indicates no significant difference.

Figure 6—figure supplement 2 continued

T2A-*rapgef4* (c) at 23 dpf. *Tg(ins:Fucci-G1)* expression is shown in red, *Tg(ins:Fucci-S/G2/M)* expression in green and CFP expression in blue. Anterior to the top. Scale bar 20 μ m. (a',b',c') Quantification of the percentage of *Tg(ins:FUCCI-S/G2/M)*-positive and *Tg(ins:FUCCI-G1)*-negative (green only) beta-cells among the CFP-positive and CFP-negative sub-populations for each experiment shown in the left-hand panels. Horizontal bars represent mean values (two-tailed t-test, $p>0.05$).

DOI: <https://doi.org/10.7554/eLife.32965.017>

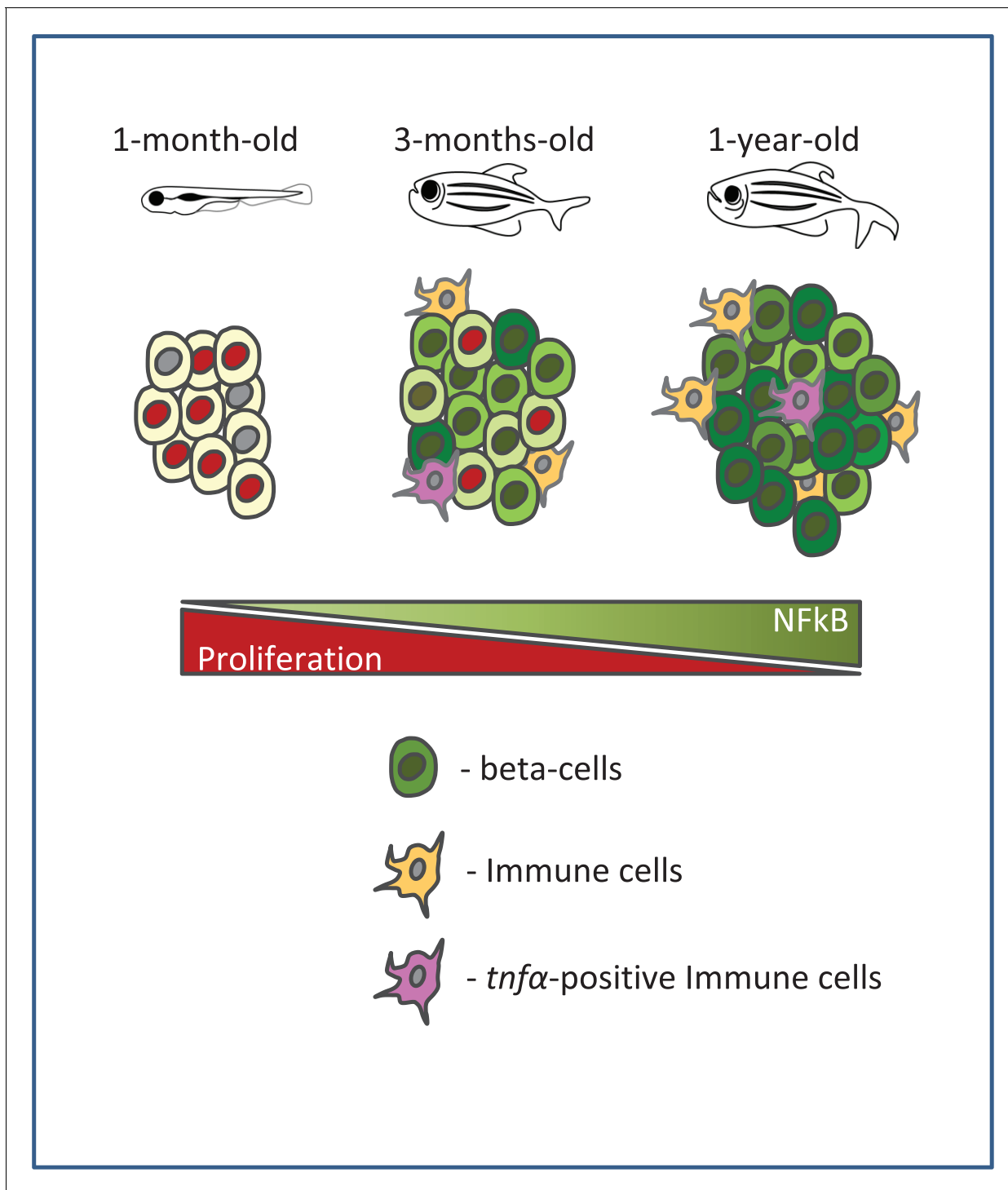


Figure 7. A schematic summarizing our model. Beta-cell proliferation declines with age together with a concurrent increase in NF- κ B signaling. The activation of NF- κ B signaling is heterogeneous among beta-cells and correlates with their proliferative heterogeneity. In particular, beta-cells with higher NF- κ B activity proliferate less compared to neighbors with lower activity, and express higher levels of *socs2*, which can inhibit beta-cell proliferation. Furthermore, the crosstalk with *tnfa*-positive immune cells in the islet provides a potential source of inflammation and NF- κ B activation in beta-cells.

DOI: <https://doi.org/10.7554/eLife.32965.019>